J Biomol NMR (2012) 52:127–139
DOI 10.1007/s10858-011-9587-0

ARTICLE

Conformational analysis by quantitative NOE measurements of the β-proton pairs across individual disulfide bonds in proteins

Mitsuhiro Takeda · Tsutomu Terauchi · Masatsune Kainosho

Received: 10 October 2011 / Accepted: 8 November 2011 / Published online: 1 December 2011

Abstract NOEs between the β-protons of cysteine residues across disulfide bonds in proteins provide direct information on the connectivities and conformations of these important cross-links, which are otherwise difficult to investigate. With conventional [U-^{13}C, ^{15}N]-proteins, however, fast spin diffusion processes mediated by strong dipolar interactions between *geminal* β-protons prohibit the quantitative measurements and thus the analyses of long-range NOEs across disulfide bonds. We describe a robust approach for alleviating such difficulties, by using proteins selectively labeled with an equimolar mixture of (2*R*, 3*S*)-[β-^{13}C; α,β-^{2}H$_2$] Cys and (2*R*, 3*R*)-[β-^{13}C; α,β-^{2}H$_2$] Cys, but otherwise fully deuterated. Since either one of the *prochiral* methylene protons, namely β2 (*proS*) or β3 (*proR*), is always replaced with a deuteron and no other protons remain in proteins prepared by this labeling scheme, all four of the expected NOEs for the β-protons across disulfide bonds could be measured without any spin diffusion interference, even with long mixing times. Therefore, the NOEs for the β2 and β3 pairs across each of the disulfide bonds could be observed at high sensitivity, even though they are 25% of the theoretical maximum for each pair. With the NOE information, the disulfide bond connectivities can be unambiguously established for proteins with multiple disulfide bonds. In addition, the conformations around disulfide bonds, namely χ^2 and χ^3, can be determined based on the precise proton distances of the four β-proton pairs, by quantitative measurements of the NOEs across the disulfide bonds. The feasibility of this method is demonstrated for bovine pancreatic trypsin inhibitor, which has three disulfide bonds.

Keywords SAIL · Disulfide connectivities · Disulfide conformation · NOEs across disulfide bonds

Introduction

The formation of disulfide bonds between correct pairs of Cys residues is essential for the proper folding and thus the biological functions of proteins with disulfide bonds. Disulfide bonds adopt specific conformations at given sites, and thereby stabilize the correct three-dimensional structure of a protein (Creighton 1984; Matsumura and Matthews 1991). In some cases, the disulfide bonds are directly involved in the biological functions of proteins (Schmidt et al. 2006; Schmidt and Hogg 2007). Therefore, determinations of the disulfide bond locations and their conformations are very important issues for understanding the structural and functional properties of proteins containing disulfide bonds. The NOEs between the β-protons of the disulfide-linked Cys pairs provide direct information for establishing the disulfide connectivity in a protein (Walewska et al. 2008). Since a Cys residue has two *prochiral* protons at the β-carbon, there should be as many as four NOEs across each disulfide bond, although not all of them can actually be observed, due to the rather long

Electronic supplementary material The online version of this article (doi:10.1007/s10858-011-9587-0) contains supplementary material, which is available to authorized users.

M. Takeda · M. Kainosho
Structural Biology Research Center, Graduate School of Science, Nagoya University, Furo-cho, Chikusa-ku, Nagoya 464-8602, Japan

T. Terauchi · M. Kainosho (✉)
Center for Priority Areas, Graduate School of Science and Technology, Tokyo Metropolitan University, 1-1 Minami-ohsawa, Hachioji 192-0397, Japan
e-mail: kainosho@tmu.ac.jp

inter-proton distances and extensive signal overlaps among other NOEs in NOESY spectra obtained for conventional [U-^{13}C, ^{15}N]-proteins.

Despite experimental difficulties, the information is very useful if one can determine the inter-proton distances between Cys β-protons across disulfide bonds, which sensitively depend on the conformation around the disulfide bond, namely χ^2 (*i*)–χ^3–χ^2 (*j*), formed between Cys (*i*) and Cys (*j*). This approach requires the accurate measurement of the cross-relaxation rates for individual proton pairs, which are obscured by the spin diffusion effects prevailing in fully protonated proteins (Kumar et al. 1981). The most serious problem is that the dipole–dipole interactions between the *geminal* protons attached to the same β-carbons give rise to very strong NOEs on their own and also facilitate problematic proton spin diffusion. These issues make quantitative NOE measurements for conformational analysis, and even a simple NOE observation for β-proton pairs across disulfide bonds for establishing the disulfide bond connectivity, quite difficult, if one uses [U-^{13}C, ^{15}N]-proteins. Recently, the replacement of sulfur by selenium, ^{77}Se, which has a half integral nuclear spin, has been proposed to determine the connectivity, by applying scalar-coupling based experiments to the diselenide bonds (Mobli et al. 2009; Mobli and King 2010). However, if the NOEs across a disulfide bond can successfully be observed in the absence of spin diffusion, it would be helpful for determining both its connectivity and conformation.

Here we present an NMR method for clearly observing the across-disulfide NOEs, by using a protein selectively labeled with newly synthesized Cys residues, (2*R*, 3*RS*)-[β-^{13}C; α,β-^{2}H$_2$] Cys in a deuterated background. This strategy is an application of the stereo-array isotope labeling (SAIL) method, which utilizes a protein with a systematically optimized isotope labeling pattern (Kainosho et al. 2006; Kainosho and Güntert 2009). The SAIL method was originally developed for the structure determination of large proteins (Kainosho et al. 2006; Kainosho and Güntert 2009), and has been providing new approaches for a variety of protein NMR studies, including the NMR analysis of aromatic ring signals, the hydrogen exchange of polar side-chain groups, solid-state NMR analysis, and fully automated protein structure determination (Takeda et al. 2009, 2010a, b, 2011; Miyanoiri et al. 2011; Takahashi et al. 2010; Ikeya et al. 2009). The important characteristic of the newly synthesized L-[β-^{13}C; $\alpha,\beta_2/\beta_3$-^{2}H$_2$] Cys is that either the β2- or β3-proton is evenly mono-deuterated. [The β2 and β3-protons in the Cys residue correspond to the pro-*S* and pro-*R* protons, respectively (Markley et al. 1998)]. When this Cys is incorporated into a disulfide-bonded protein, four isotopomers are generated in each disulfide bond. In this case, while the geminal interaction within the methylene proton is eliminated, the four combinations of Cys β-protons across the disulfide bond are certainly formed in all four of the isotopomers. The observation of the multiple across-disulfide NOEs results in the definitive determination of the disulfide connectivity, and the inter-proton distances derived from the four across-disulfide NOEs are helpful to determine the conformations of disulfide bonds.

We applied this method to the three disulfide bonds (Cys5–Cys55, Cys14–Cys38 and Cys30–Cys51) in a 6.5 kDa protein, bovine pancreatic trypsin inhibitor (BPTI). Although BPTI is relatively small, it contains various important features of proteins, and thus has long been an interesting and important subject of NMR studies (Berndt et al. 1992; Otting et al. 1993; Skalicky et al. 2001; Wagner 1983). The three disulfide bonds in BPTI are suitable and interesting targets for testing our approach for the following two reasons: First, its high-resolution crystal structure has been solved, and thus precise information on the disulfide conformations is available (Wlodawer et al. 1984). Second, it includes a disulfide bond that exists in a dynamic equilibrium (Otting et al. 1993; Szyperski et al. 1993; Grey et al. 2003; Shaw et al. 2010). In this equilibrium, the high-populated major conformation (*M*) exchanges with either of two very low-populated conformations, m_{c14} and m_{c38}, through the Cys14 χ^1 and Cys38 χ^1 rotameric conversions, respectively (i.e., $m_{c14} \leftarrow \rightarrow M \leftarrow \rightarrow m_{c38}$), and the exchange rate between *M* and m_{c14} is about 30-fold faster than that between *M* and m_{c38} (Otting et al. 1993; Grey et al. 2003). In this report, we will focus on the feasibility of our approach for defining the disulfide bonds of BPTI.

Materials and methods

Computation of distances between β-protons in a disulfide bond

The inter-proton distances for the four cysteine β-proton pairs across a disulfide bond, as a function of χ^2 (*i*), χ^3 and χ^2 (*j*), were computed using the Matlab software (MathWorks Inc., Natick, MA, USA), according to the previously described procedure (Billeter et al. 1982). In this computation, the bond lengths and bond angles were fixed (See Supporting information). The χ^3 angles were fixed to +90° or −90°, which are the predominant vales in actual protein disulfide bonds, and χ^2 (*i*) and χ^2 (*j*) were set as variable parameters. The calculated distances are displayed as contour lines in the χ^2 (*i*)–χ^2 (*j*) planes.

Chemical syntheses of L-[β-^{13}C; $\alpha,\beta_2/\beta_3$-^{2}H$_2$] cysteine; i.e., (2*R*, 3*RS*)-[3-^{13}C; 2,3-^{2}H$_2$] cysteine

The L-[β-^{13}C; $\alpha,\beta_2/\beta_3$-^{2}H$_2$] Cys was prepared by mixing L-[β-^{13}C; α,β_2-^{2}H$_2$] Cys **1** and L-[β-^{13}C; α,β_3-^{2}H$_2$] Cys **2**.

Both labeled cysteines are synthesized using (2*S*, 3*R*)-[3-^{13}C; 2,3-$^{2}H_2$] Ser **3** as the key intermediate, starting from potassium [^{13}C] cyanide **4,** by a previously reported method (Terauchi et al. 2008). Thus, the dehydroserine derivative **5**, prepared from potassium [^{13}C] cyanide **4**, was subjected to reduction using deuterium gas in the presence of (S,S)-Et-DuPHOS-Rh, followed by hydrolysis with MeOH/conc. HCl at room temperature for 6 h, and then 6 N DCl at 110°C for 6 h to give (2*S*, 3*R*)-[3-^{13}C; 2,3-$^{2}H_2$] Ser **3**. For the synthesis of L-[β-^{13}C; α,β_2-$^{2}H_2$] Cys **1**, Ser **3** was converted to the tosylated derivative **8**, and then subjected to thioacetylation by potassium thioacetate, to yield the deuterium-labeled cysteine derivative, followed by deprotection by refluxing with 6 N DCl and purification by Dowex 50W-X8 column chromatography, to give L-(2*R*, 3*S*)-[3-^{13}C; 2,3-$^{2}H_2$] Cys–HCl, namely L-[β-^{13}C; α,β_2-$^{2}H_2$] Cys–HCl **1**. The deuterium enrichment of the $H_{\beta 2}$ of the Cys **1** is 99.3% D. For the synthesis of L-[β-^{13}C; α,β_3-$^{2}H_2$] Cys **2**, we followed the scheme developed by Arnold et al. (1985, 1988), Ramer et al. (1986), using (2*S*, 3*R*)-[3-^{13}C; 2,3-$^{2}H_2$] Ser **3**. As a result, we accomplished the synthesis of L-[β-^{13}C; α,β_3-$^{2}H_2$] Cys–HCl **2**. The deuterium enrichment of the $H_{\beta 3}$ of Cys **2** is 99.3% D (Scheme 1).

Sample preparation

The BPTI proteins for NMR analyses were prepared according to the previously reported method (Altman et al. 1991). In this study, *E. coli* strain BL21 (DE3) cells were transformed with the expression vector encoding the BPTI protein fused with a Z-domain at its N-terminus. The transformed cells were selected on LB agar plates with 100 μg/mL ampicillin. The *E. coli* cells were then cultured at 37°C in 50 mL of H_2O/M9 medium (3.4 g/L Na_2HPO_4 (anhydrous), 0.5 g/L KH_2PO_4 (anhydrous), 0.25 g/L NaCl, 5 g/L [U-^{2}H] D-glucose, 0.5 g/L NH_4Cl, 0.5 mg/L thiamine, 0.03 mM $FeCl_3$, 0.05 mM $MnCl_2$, 0.1 mM $CaCl_2$ and 1 mM $MgSO_4$) containing 2 g/L [U-^{2}H] algal amino acid mixture (Chlorella Industry Co. Ltd., Tokyo, Japan), 50 mg/L unlabeled Cys and 50 mg/L unlabeled Trp. When the culture reached an OD_{600} of 0.4–0.6, the *E. coli* cells were collected and resuspended in 500 mL of D_2O/M9 medium containing [U-^{2}H, 99%] algal amino acid mixture, 50 mg/L unlabeled Cys and 50 mg/L unlabeled Trp. The *E. coli* cells were then cultured in the D_2O/M9 medium at 37°C with shaking. When the OD_{600} reached 0.5, the cells were collected by centrifugation and resuspended in 500 mL of D_2O/M9 medium, containing 2 g/L [U-^{2}H] algal amino acid mixture, 12 mg/L L-[β-^{13}C; $\alpha,\beta_2/\beta_3$-$^{2}H_2$] Cys–HCl (corresponding to 10 mg of Cys) and 50 mg/L unlabeled Trp, and then isopropyl-β-D-thiogalactopyranoside (IPTG) was added to a final concentration of 0.4 mM. The protein production was induced for 4–5 h, and then the cells were collected by centrifugation.

The fusion protein was produced as an insoluble inclusion body. The *E. coli* cells were suspended in 100 mL of lysis buffer [10 mM Tris-HCl (pH 8.0), 1 mM EDTA, 0.5% Triton X-100 and 1 mM dithiothreitol (DTT)], and then disrupted by ultrasonication. The precipitate was dissolved in 25 mL of dissolving buffer (10 mM Tris-HCl (pH 8.0), 7 M guanidine hydrochloride and 1 mM DTT) and stirred for 10 min at room temperature (about 25°C). DTT was then added to a final concentration of 100 mM, and the mixture was stirred for 1 h. After centrifugation at 1,600×*g* for 20 min, the supernatant was dialyzed against 2 L of a solution containing 10 mM HCl and 10 mM DTT for 5 h, using a dialysis membrane with a molecular weight cut-off of 6,000–8,000 Da. The solution was then centrifuged at 1,000×*g* for 20 min at 4°C. Refolding buffer (300 mL; 100 mM Tris-HCl (pH 8.7), 10 mM reduced glutathione, 1 mM oxidized glutathione, 200 mM KCl and 1 mM EDTA) was then added to 35 mL of the supernatant. (The amount varied, depending on the volume of the supernatant.) The mixed solution was then applied to a chymotrypsin-bound Affi-gel column. The flow-through fraction was reapplied to the column, to ensure the binding of the target protein. The column was then washed with 25 mL of equilibration buffer (100 mM triethanolamine

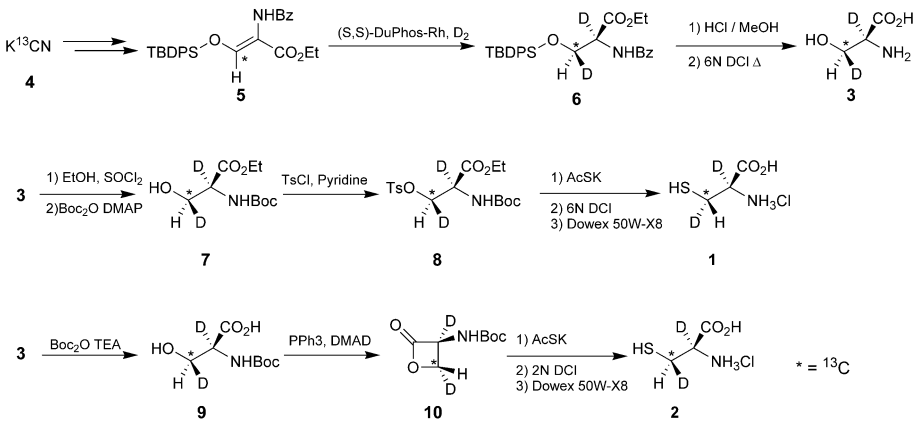

Scheme 1 Chemical syntheses of (2*R*, 3*RS*)-[3-^{13}C; 2,3-$^{2}H_2$] Cys, i.e. L-[β-^{13}C; $\alpha,\beta_2/\beta_3$-$^{2}H_2$] Cys

(pH 7.8), 300 mM NaCl and 10 mM $CaCl_2$). Afterwards, one column volume of the elution buffer was applied, and the column was incubated overnight at 4°C. The cleaved tag was eluted by two column volumes of equilibration buffer, and then the BPTI protein was eluted with elution buffer [500 mM KCl, 10 mM HCl (pH 2.1)]. The eluted sample was concentrated, and its pH was adjusted to 7.0. The correctly folded BPTI monomer was separated by gel-filtration chromatography in running buffer (10 mM NaPi (pH 7.0) and 150 mM NaCl). The fraction corresponding to the BPTI monomer was collected and concentrated. During this step, the buffer was exchanged to a solution containing 5 mM NaCl. Finally, the solution was lyophilized and then diluted into a D_2O solution. The proportion of Cys incorporation was evaluated based on the effective concentration, which was determined, based on the peak intensity of $^{13}C_\beta$ in the ^{13}C 1D NMR spectrum, to be 0.7 mM, and the total concentration, determined by UV absorption at 280 nm, was 1.0 mM. In addition, a fully protonated BPTI containing L-[α,β-$^{13}C_2$; β_2-^{2}H] Cys residues was produced by the same procedure.

NMR measurements and analysis of cross-relaxation rates

NNR experiments were performed using an Avance 600 spectrometer equipped with a TCI cryogenic probe (Bruker Biospin), unless stated otherwise. All spectra were processed and analyzed by the Topspin software (Bruker Biospin).

^{1}H-^{13}C HSQC experiments on the (L-[β-^{13}C; $\alpha,\beta_2/\beta_3$-$^2H_2$] Cys, [U-^{2}H])-labeled BPTI and the L-[α,β-$^{13}C_2$; β_2-^{2}H] Cys-labeled BPTI were acquired with ^{2}H decoupling during t_1 chemical shift encoding on the ^{13}C atom. The data points and the spectral width of the ^{1}H-^{13}C HSQC experiments were 256 (t_1) × 1,024 (t_2) points and 6,000 Hz (ω_2, ^{13}C) × 8,000 Hz (ω_1, ^{1}H), respectively. The carrier frequency of carbon was set to 40 ppm. The number of scans/FID was 16 for the (L-[β-^{13}C; $\alpha,\beta_2/\beta_3$-$^2H_2$] Cys, [U-^{2}H])- and L-[α,β-$^{13}C_2$; β_2-^{2}H] Cys-labeled samples and 32 for the [U-^{13}C, ^{15}N] Cys (UL-Cys)-labeled sample. The stereo-assignment of the cysteine β-protons was performed with the spectral pattern of the L-[α,β-$^{13}C_2$; β_2-^{2}H] Cys-labeled BPTI. ^{1}H-^{13}C constant-time HSQC experiments on the UL-Cys-labeled BPTI were performed using the same parameters as those for the L-[α,β-$^{13}C_2$; β_2-^{2}H] Cys-labeled BPTI. The data points and the spectral width of the ^{13}C-edited [^{1}H, ^{1}H] NOESY on the (L-[β-^{13}C; $\alpha,\beta_2/\beta_3$-$^2H_2$] Cys, [U-^{2}H])-labeled BPTI samples were 512 (t_1) × 1,024 (t_2) points and 6,600 Hz (ω_1, ^{1}H) × 6,600 Hz (ω_2, ^{1}H), respectively. Given that the optimal repetition time is 1.25 × T_1 (longitudinal relaxation time), the repetition times were set to 5.3 and 1.5 s for (L-[β-^{13}C; $\alpha,\beta_2/\beta_3$-$^2H_2$] Cys, [U-^{2}H])-labeled BPTI and UL-Cys-labeled BPTI, respectively. The carrier frequency of carbon was set to 40 ppm.

The cross-relaxation rates for the across-disulfide NOEs were evaluated by fitting the peak heights of the across-disulfide NOEs as a function of the mixing times, using the equations described by Vögeli et al. (2009, 2010). The fitting was performed with the Matlab software (MathWorks Inc., Natick, MA, USA). First, the auto-relaxation rates were determined, using the equation:

$$I = I_0 \exp(-\rho t), \quad (1)$$

where I is the observed peak intensity of the auto-peak, I_0 is the initial peak intensity, ρ is the value of the auto-relaxation rate and t is the value of the NOE mixing time. Subsequently, the values of the cross-peak intensity over the initial peak height were fitted, using the equation:

$$I/I_0 = -\sigma\left(t + 0.5\rho t^2\right), \quad (2)$$

where I is the observed peak intensity of the cross-peak, I_0 is the initial peak intensity, ρ is the value of the auto-relaxation rate, σ is the cross-relaxation rate and t is the mixing time. Here, considering that the effective concentrations for the auto-peak and the cross-peak are one-half and one-fourth of the actual concentrations, respectively, and the labeling efficiency of Cys was 70 ± 5%, the experimental value of I/I_0 was scaled by 2.9 [= 1/(0.5 × 0.7)]. The fitting of a model curve to the measured data points was performed by nonlinear least-squares fitting, and the determined values were defined as the mean values. The error values were then evaluated using the Monte Carlo method, in which 50 iterations of curve fitting were performed for the defined mean values plus randomly generated errors, and the error values were defined as the standard deviation between the values.

The evaluation of ^{13}C T_1 and T_2 on the (L-[β-^{13}C; $\alpha,\beta_2/\beta_3$-$^2H_2$] Cys, [U-^{2}H])-labeled BPTI sample was performed following established procedures (Kay et al. 1989; Peng and Wagner 1992). The evaluation was performed for both the $^{13}C_\beta$(-$^1H_{\beta2}$) and $^{13}C_\beta$(-$^1H_{\beta3}$) pairs on a residue-by-residue basis. During inversion, a train of proton inversion pulses was applied to eliminate the effect of dipole-CSA cross correlated relaxation (Boyd et al. 1990).

The evaluation of ^{1}H T_1 was performed by a ^{1}H inversion recovery experiment for the UL-Cys-labeled BPTI and the (L-[β-^{13}C; $\alpha,\beta_2/\beta_3$-$^2H_2$] Cys, [U-^{2}H])-labeled BPTI at 14.1 and 23.2 T, respectively [Avance 900 spectrometer equipped with a TCI cryogenic probe (Bruker Biospin)]. As the recovery curves were almost the same between the different H_β protons, the evaluation was performed for the Cys5 $H_{\beta3}$ protons as a representative.

The conversion of the cross-relaxation rates into the inter-proton distances was performed using the following equation (Cavanagh et al. 2007; Vögeli et al. 2009):

$$\sigma = \frac{\hbar^2 \mu_0 \gamma^4 \tau_c}{160\pi^2 r^6}, \quad (3)$$

where r is the effective distance, σ is the cross-relaxation rate, $\hbar$ is Planck's constant, μ_0 is the permeability in a vacuum, τ_c is the rotational correlation time of the molecule, and γ is the gyromagnetic ratio of a proton.

Results and discussion

In a disulfide bond formed between the *i*th and *j*th Cys residues, four pairs of β-protons exist, for which the across-disulfide NOEs are observed [i.e., $H_{\beta2}(i)$–$H_{\beta2}(j)$, $H_{\beta2}(i)$–$H_{\beta3}(j)$, $H_{\beta3}(i)$–$H_{\beta2}(j)$ and $H_{\beta3}(i)$–$H_{\beta3}(j)$]. In most cases, a disulfide bond adopts either a right- ($\chi^3 = \sim +90^\circ$) or left-handed ($\chi^3 = \sim -90^\circ$) conformation (Richardson 1981; Ozhogina and Bominaar 2009), and thus the inter-proton distances of the four β-proton pairs vary depending on the χ^2 (i) and χ^2 (j) dihedral angles (Fig. 1).

A key part of our strategy is to create a situation where the four across-disulfide NOEs are observed simultaneously, in the complete absence of the spin diffusion effect. In the case of [U-^{13}C, ^{15}N] labeled proteins, ^{1}H-^{1}H dipole interactions, especially between geminal protons [i.e., $H_{\beta2}(i)$–$H_{\beta3}(i)$ and $H_{\beta2}(j)$–$H_{\beta3}(j)$], cause deleterious proton spin diffusion and may result in signal overlaps with the across-disulfide NOEs. To overcome this issue, we designed and synthesized L-[β-^{13}C; α,β_2/β_3-^{2}H$_2$] Cys. In this Cys residue, only the β-carbon is enriched by ^{13}C, and either the β2- or β3-proton is evenly mono-deuterated. This Cys can be regarded as the equimolar mixture of (2*R*, 3*S*)-[3-^{13}C; 2,3-^{2}H$_2$] Cys (L-[β-^{13}C; α,β_2-^{2}H$_2$] Cys) and (2*R*, 3*R*)-[3-^{13}C; 2,3-^{2}H$_2$] Cys (L-[β-^{13}C; α,β_3-^{2}H$_2$] Cys) (Fig. 2). (The pro-*R* and pro-*S* protons are labeled with β3 and β2, respectively.) The incorporation of L-[β-^{13}C; α,β_2/β_3-^{2}H$_2$] Cys into a target protein leads to the generation of four equally populated isotopomers, namely $^1H_{\beta2}/^2H_{\beta3}$ (i)–$^1H_{\beta2}/^2H_{\beta3}$ (j), $^1H_{\beta2}/^2H_{\beta3}$ (i)–$^2H_{\beta2}/^1H_{\beta3}$ (j), $^2H_{\beta2}/^1H_{\beta3}$ (i)–$^1H_{\beta2}/^2H_{\beta3}$ (j) and $^2H_{\beta2}/^1H_{\beta3}$ (i)–$^2H_{\beta2}/^1H_{\beta3}$ (j). In each of the four isotopomers, the across-disulfide NOE is observed for one β-proton pair (Fig. 3). In addition, the surrounding protons are perdeuterated, such that the proton spin diffusion is completely eliminated.

Preparation of BPTI selectively labeled by Cys in a deuterated background

To examine the feasibility of the proposed approach, a perdeuterated BPTI protein selectively labeled with L-[β-^{13}C; α,β_2/β_3-^{2}H$_2$] Cys was prepared, according to a previously described procedure (Altman et al. 1991).

In this study, the BPTI protein selectively labeled with Cys was produced by using an autotrophic *E. coli* strain, BL21 (DE3) (Novagen), as in conventional amino-acid selective labeling (Muchmore et al. 1989; Waugh 1996). The BL21 (DE3) strain is endowed with a robust protein production system, and thus is the most widely used for recombinant protein preparation. A potential concern with the use of an autotrophic *E. coli* cell is that the label incorporation may be low, which would decrease the intensity of the NMR peaks relative to that expected from the sample concentration. Especially, in terms of observing across-disulfide NOEs, excessively low label incorporation is problematic, as across-disulfide NOEs involve two Cys residues and thus their peak intensities are proportional to the square of the Cys label incorporation. In the present case, by adding 10 mg of isotope labeled Cys into 500 mL of D_2O M9 medium prior to IPTG induction, 70% label incorporation was achieved (data not shown).

The label incorporation can be improved by increasing the amount of Cys supplemented in the *E. coli* culture, but caution should be used, since Cys may exert an inhibitory effect on the growth of *E. coli* cells in minimal media (Roberts et al. 1957; Kari et al. 1971). In our experiments, a slower growth rate was observed for *E. coli* BL21 (DE3) cells (data not shown). As the growth inhibitory effect of Cys can be mitigated by additional supplementation with leucine, isoleucine, threonine and valine residues, it is assumed that cysteine interferes with the biosynthesis of these amino acids (Kari et al. 1971). In this regard, the supplementation of the culture medium with the commercially available deuterated algal hydrolysate is practically useful, since the algal hydrolysate contains the four amino acids, and is presently relatively cheaper than the four individual deuterated amino acids. Fortunately, the algal hydrolysate usually does not contain Cys (and Trp), due to the hydrolysis process, and thus its use does not decrease the labeling efficiency of Cys.

In terms of the incorporation of the isotope labeled Cys residue, the use of an *E. coli* cysteine auxotrophic strain, such as the JM15 strain (LeMaster 1996), which is available from the *E. coli* Genetic Stock Center (http://cgsc.biology.yale.edu/), or a cell-free expression system (Torizawa et al. 2004; Takeda et al. 2007) promises high incorporation. One problem with the JM15 strain is that its growth is likely to be slower than that of BL21 (DE3) cells. In such a situation, the supplementation with the algal hydrolysate is quite important to mitigate the inhibition by Cys and achieve an acceptable production level of the target protein. On the other hand, the issue in the conventional cell-free system is that the target proteins are produced in a reducing environment, and thus some modifications may be needed

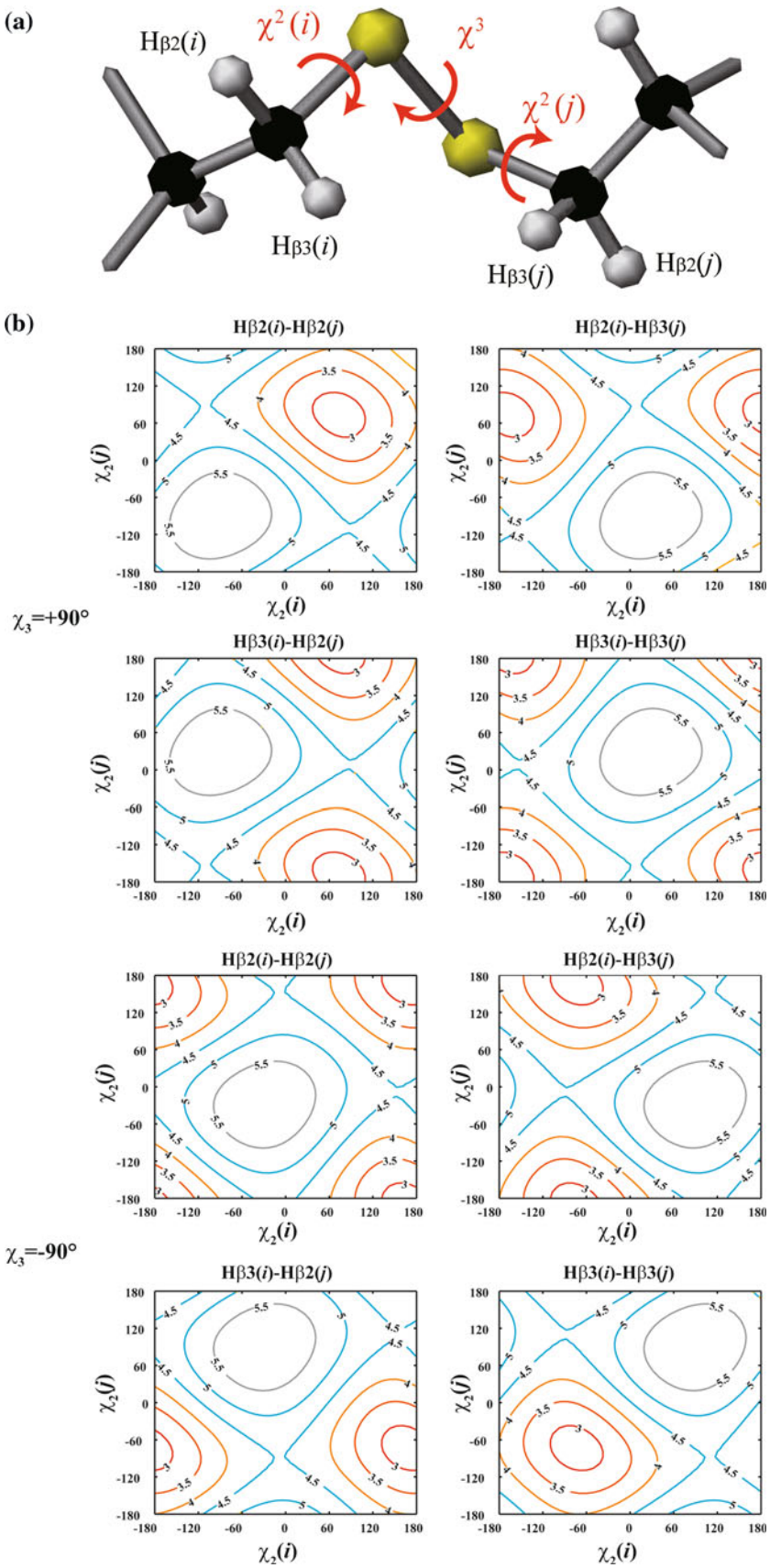

Fig. 1 The conformation of a disulfide bond is defined by three dihedral angles, χ^2 (*i*), χ^3 and χ^2 (*j*) (**a**). The four inter-proton distances between the β-protons of two disulfide-linked Cys residues are depicted as *contour lines* in the $\chi^2(i)$–$\chi^2(j)$ plane at χ^3 angles of +90° and −90°, the predominant values in actual cases (**b**). These *contour lines* were computed by assuming fixed bond lengths and angles

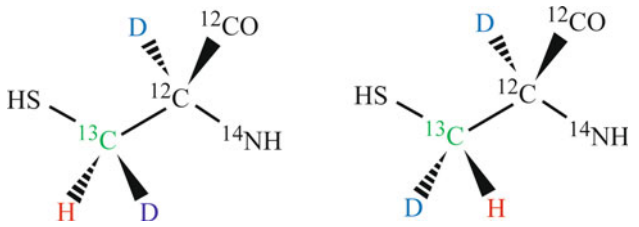

Fig. 2 Chemical structures of (2*R*, 3*R*)-[3-^{13}C; 2,3-^{2}H$_2$] Cys, i.e. L-[β-^{13}C; α,β_3-^{2}H$_2$] Cys (*left*), and (2*R*, 3*S*)-[3-^{13}C; 2,3-^{2}H$_2$] Cys, i.e. L-[β-^{13}C; α,β_2-^{2}H$_2$] Cys (*right*). (2*R*, 3*RS*)-[3-^{13}C; 2,3-^{2}H$_2$] Cys, i.e. L-[β-^{13}C; α,β_2/β_3-^{2}H$_2$] Cys, is a 1:1 mixture of these two labeled cysteines

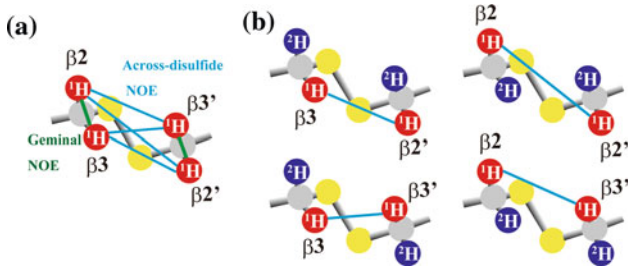

Fig. 3 Schematic representation of the NOEs observed for a disulfide bond in proteins selectively labeled with UL-Cys (**a**) and L-[β-^{13}C; α,β_2/β_3-^{2}H$_2$] Cys (**b**). ^{1}H, ^{2}H, carbon and sulfur atoms are colored *red*, *blue*, *gray* and *yellow*, respectively. Across-disulfide NOEs (*cyan*) and geminal NOEs (*green*) are depicted as *lines*. In **b**, the geminal NOE is absent and the across-disulfide NOE is observed for one of the four isotopomers

for expressing disulfide-containing proteins (Goerke and Swartz 2008).

The isotope labeling pattern of the prepared sample was confirmed by its ^{1}H-^{13}C HSQC spectrum. The ^{1}H-^{13}C HSQC spectra of the UL-Cys-, (L-[β-^{13}C; α,β_2/β_3-^{2}H$_2$] Cys, [U-^{2}H])- and L-[α,β-^{13}C$_2$; β_2-^{2}H] Cys-labeled BPTI samples are shown in Fig. 4a, b and c, respectively. The stereo-assignments of the ^{1}H$_\beta$-^{13}C$_\beta$ correlation peaks in the UL-Cys- and (L-[β-^{13}C; α,β_2/β_3-^{2}H$_2$] Cys, [U-^{2}H])-labeled samples were performed by comparing their peak positions with those of the L-[α,β-^{13}C$_2$; β_2-^{2}H] Cys-labeled sample (Fig. 4c). The spectral patterns of the UL-Cys- and L-[β-^{13}C; α,β_2/β_3-^{2}H$_2$] Cys-labeled BPTI proteins appear identical, but their chemical shifts are slightly different in both the ^{1}H and ^{13}C dimensions (Fig. 4d). The chemical shifts of ^{1}H$_{\beta3}$ and ^{13}C$_\beta$ in L-[β-^{13}C; α,β_2/β_3-^{2}H$_2$] Cys were almost identical to those in the L-[α,β-^{13}C$_2$; β_2-^{2}H] Cys-labeled protein. In addition, in the [^{1}H, ^{2}H] decoupled ^{13}C 1D experiments, no β-carbon signal due to either the CH$_2$ or CD$_2$ species was detected next to that due to the CHD species (data not shown). These results confirmed the mono-deuteration of the methylene groups in the (L-[β-^{13}C; α,β_2/β_3-^{2}H$_2$] Cys, [U-^{2}H])-labeled sample. Note that the line-widths of the methylene protons in the (L-[β-^{13}C; α,β_2/β_3-^{2}H$_2$] Cys, [U-^{2}H])- and the L-[α,β-^{13}C$_2$; β_2-^{2}H] Cys-labeled samples are sharper than those in the UL-Cys-labeled BPTI, due to the elimination of dipole interactions and long-range scalar couplings (Fig. 4e). It is noteworthy that, as the β-carbon is not adjacent to the ^{13}C atom in L-[β-^{13}C; α,β_2/β_3-^{2}H$_2$] Cys, the chemical shift encoding was performed without the constant time technique, thus enhancing the signal sensitivity.

Observation and analysis of across-disulfide NOEs

With the hope of observing quantitative across-disulfide NOEs, ^{13}C-edited [^{1}H, ^{1}H] NOESY spectra with different mixing times, from 50 to 500 ms, were acquired at 10°C for the sample of (L-[β-^{13}C; α,β_2/β_3-^{2}H$_2$] Cys, [U-^{2}H])-labeled BPTI. For comparison, the same NOESY experiments were also performed for a sample of UL-Cys-labeled BPTI.

One caution that should be taken is that the longitudinal relaxation time (T_1) of ^{1}H is longer than that of a protonated protein. The T_1 of a cysteine β-proton in the (L-[β-^{13}C; α,β_2/β_3-^{2}H$_2$] Cys, [U-^{2}H])-labeled BPTI was 1.5–2 times longer than that in the UL-Cys-labeled protein (Table S1). In the (L-[β-^{13}C; α,β_2/β_3-^{2}H$_2$] Cys, [U-^{2}H])-labeled BPTI, the spin relaxation pathway was limited to the dipole interaction with the attached carbon. In actual practice, the observed T_1 value is very close to that back-calculated from the overall correlation time of BPTI for an isolated ^{1}H-^{13}C spin pair (data not shown).

By virtue of the extensive deuteration, the NOE peaks other than the across-disulfide NOEs of interest are eliminated in the (L-[β-^{13}C; α,β_2/β_3-^{2}H$_2$] Cys, [U-^{2}H])-labeled protein (Fig. 5). Especially, the elimination of the intense geminal NOEs in the (L-[β-^{13}C; α,β_2/β_3-^{2}H$_2$] Cys, [U-^{2}H])-labeled protein substantially clarified the appearance of the NOESY spectrum. If needed, the diagonal peak suppression developed by Wu et al. (2004) can also be applied, due to its methine (CHD), rather than methylene (CH$_2$), spin system.

The successful observation of the across-disulfide NOEs led to the determination of the disulfide bonded partners. In this case, the across-disulfide NOEs were observed between the β-protons of Cys5 and Cys55, Cys14 and Cys38, and Cys30 and Cys51, which coincided with the disulfide connectivities in the crystal structure of BPTI.

We highly recommend checking all four of the across-disulfide NOEs. Mobli and coworkers pointed out a case where two different disulfide bonds are coincidentally located in spatial proximity to each other, and the inter-disulfide NOEs between the β-protons of different disulfide bonds are thus mistakenly identified as across-disulfide NOEs (Mobli et al. 2009; Mobli and King 2010). Even in such a case, since the across-disulfide NOEs are certainly

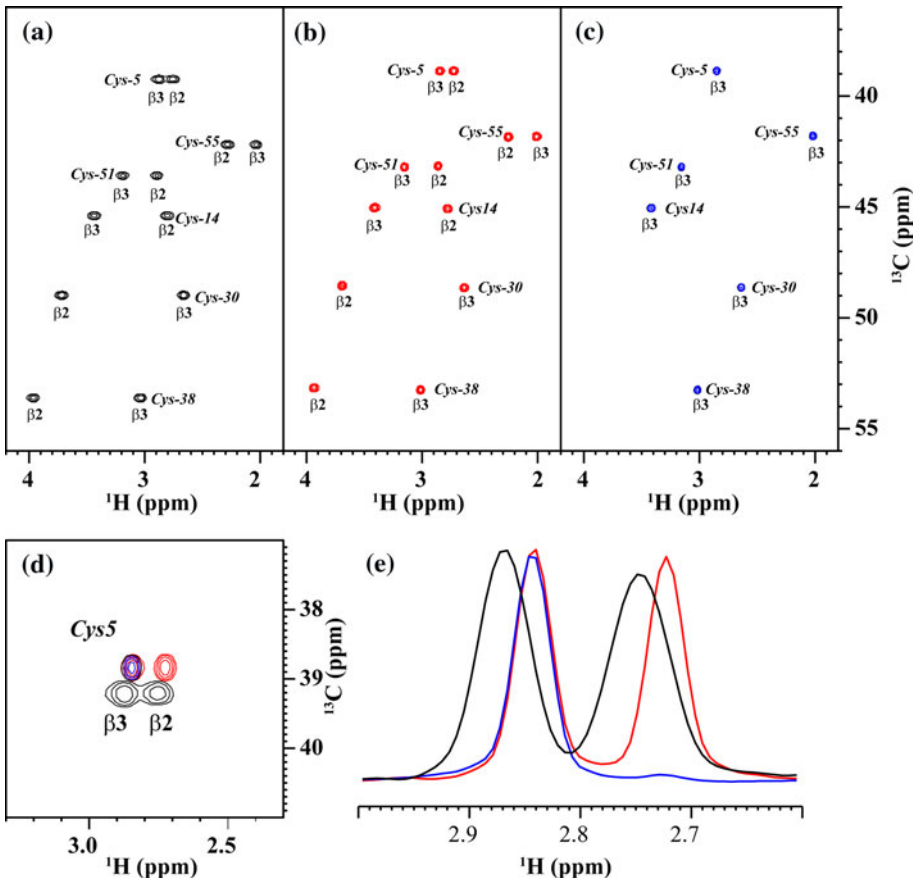

Fig. 4 ^{1}H-^{13}C HSQC spectra of UL-Cys-labeled BPTI (**a**), (L-[β-^{13}C; α,β_2/β_3-$^{2}H_2$] Cys, [U-^{2}H])-labeled BPTI (**b**) and L-[α,β-$^{13}C_2$; β_2-^{2}H] Cys-labeled BPTI (**c**). Peaks are labeled with their residue and stereo-assignment. The observed chemical shift of $^{13}C_\beta$ for the (L-[β-^{13}C; α,β_2/β_3-$^{2}H_2$] Cys, [U-^{2}H])-labeled sample is almost identical to that of the L-[α,β-$^{13}C_2$; β_2-^{2}H] Cys-labeled protein, but is different from that of the UL-Cys-labeled sample, which ensures the mono-deuteration at the β-position (**d**). The ^{1}H slices of the Cys5 resonances (**e**). For clarity, the spectra of the UL-Cys-labeled BPTI, (L-[β-^{13}C; α,β_2/β_3-$^{2}H_2$] Cys, [U-^{2}H])-labeled BPTI and L-[α,β-$^{13}C_2$; β_2-^{2}H] Cys-labeled BPTI are colored *black*, *red* and *blue*. These spectra were acquired using an Avance 600 spectrometer equipped with a TCI cryogenic probe at 10°C

observable, this checking procedure reduces the possibility of misinterpretation.

One may wonder whether this approach would work in a protein selectively labeled with L-[β-^{13}C; α,β_2/β_3-$^{2}H_2$] Cys in a protonated, rather than deuterated, background. In our test, this kind of sample can be used to identify the connectivity of a disulfide bond. The elimination of the geminal NOE greatly simplifies the NOESY spectrum, and it can be used for determining the disulfide connectivity. However, the spin diffusion and the overlap with the NOEs from the surrounding protons hamper the quantitative estimation of the cross-peaks (Fig. S1 and S2).

Another key aspect of our approach is the elimination of the proton spin diffusion. A comparison of the NOE build-up curves between the UL-Cys-labeled BPTI and (L-[β-^{13}C; α,β_2/β_3-$^{2}H_2$] Cys, [U-^{2}H])-labeled BPTI revealed that the peak intensity started to drop at a mixing time of 200 ms in the former, but it persisted even at a mixing time of 500 ms in the latter (Fig. 6). It should be pointed out that the peak intensities of the NOE cross-peaks at symmetrical positions [i.e., H(i)($F1$) > H(j)($F2$) and H(j)($F1$) > H(i)($F2$)] are not identical in the UL-Cys-labeled BPTI, but are identical in the (L-[β-^{13}C; α,β_2/β_3-$^{2}H_2$] Cys, [U-^{2}H])-labeled protein (e.g., compare red lines in Fig. 5). The different intensities of the NOE peaks in the protonated protein arise from the different magnitudes of the spin relaxation pathways between Cys5 and Cys55. In the case of the (L-[β-^{13}C; α,β_2/β_3-$^{2}H_2$] Cys, [U-^{2}H])-labeled BPTI, on the other hand, the peak intensities at symmetrical positions are almost identical, due to the background deuteration (Fig. 5b).

The cross-relaxation rates of the across-disulfide NOEs were evaluated by curve-fitting. For the NOESY build-up curves of the (L-[β-^{13}C; α,β_2/β_3-$^{2}H_2$] Cys, [U-^{2}H])-labeled BPTI, its peak intensities over the range from 50 to 500 ms were fitted as a function of the mixing times to the expressions of Vögeli et al. (2009) (Fig. 7a). In the fitting procedure, the cross-peak intensities were corrected by considering the following two factors. First, the disulfide bond composed of L-[β-^{13}C; α,β_2/β_3-$^{2}H_2$] Cys is a mixture of four isotopomers, and diagonal peaks are observed for two of them, while a cross-peak is observed for one of them (Fig. 3b). Second, the intensity of the across-disulfide NOE is proportional to the square of the Cys label incorporation, because the across-disulfide NOE involves two different Cys residues.

The determined cross-relaxation rates were then converted to the effective distances under the assumption of a rigid molecule (i.e., the absence of internal motion). For this purpose, the overall correlation time of BPTI was

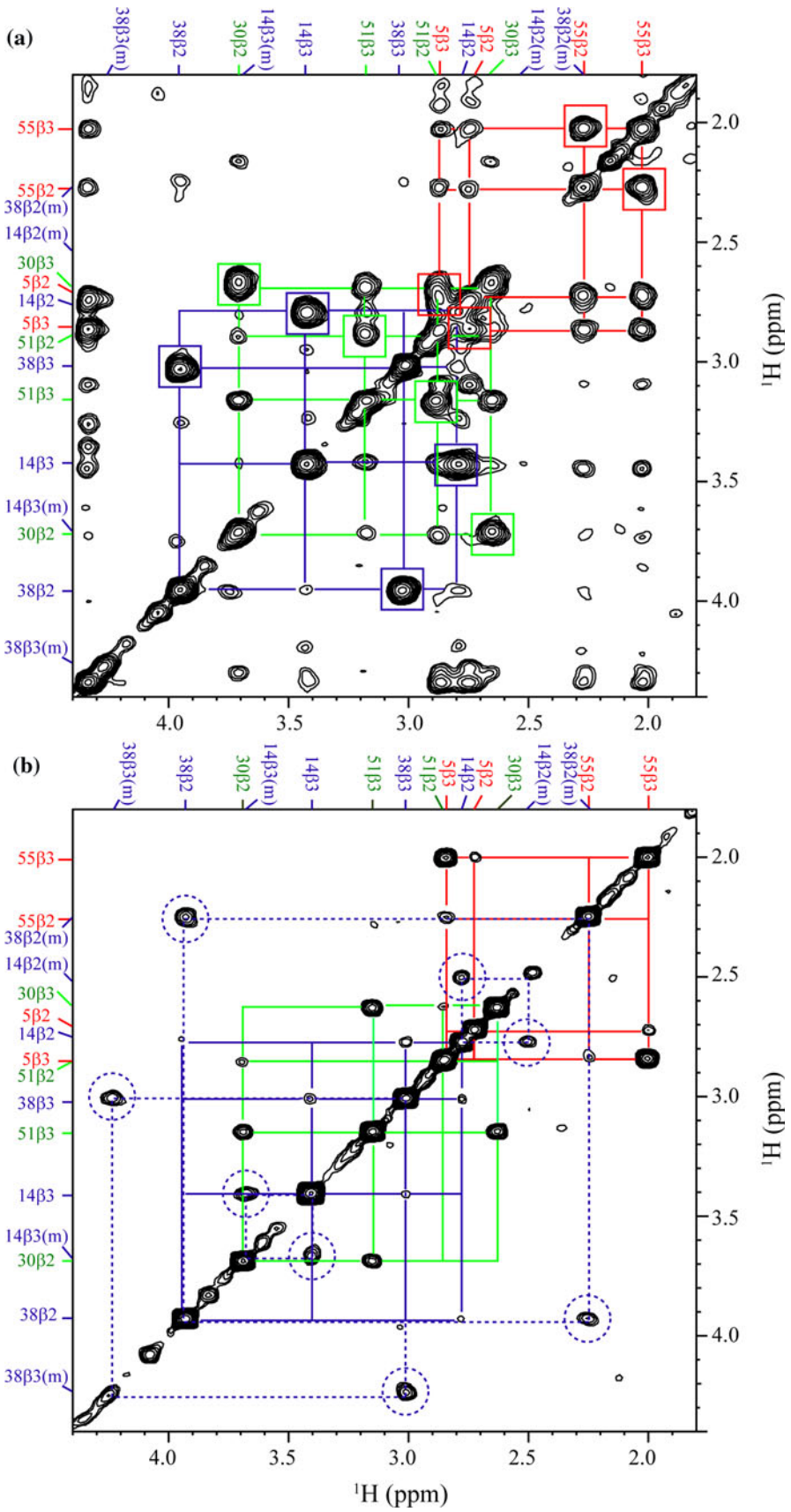

Fig. 5 Comparison of the 2D ^{13}C-edited [^{1}H, ^{1}H] NOESY for the UL-Cys-labeled BPTI (**a**) and the (L-[β-^{13}C; α,β_2/β_3-$^{2}H_2$] Cys, [U-^{2}H])-labeled BPTI (**b**). Both spectra were acquired at a mixing time of 400 ms, with a 1.0 mM sample concentration. The spectra were acquired at 10°C, using an Avance 600 spectrometer equipped with a TCI cryogenic probe. The assignments are labeled on their axis at the *upper* and *left* positions. The peaks belonging to the Cys5–Cys55, Cys14–Cys38 and Cys30–Cys51 disulfide bonds are each connected by *red*, *blue* and *green lines*, respectively. The geminal NOEs are *boxed*. In **b**, the exchange-peaks are connected by *dashed lines*

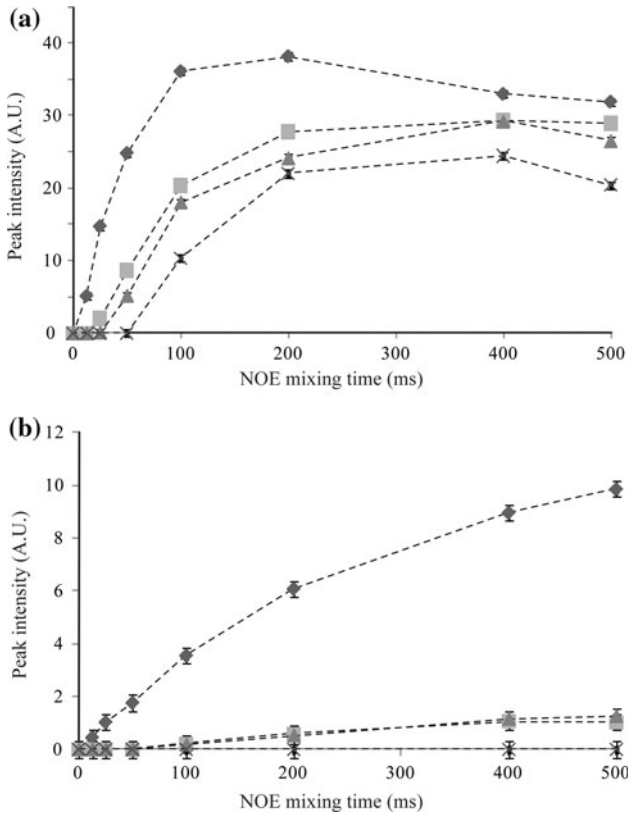

Fig. 6 NOE build-up curves of the four across-disulfide NOEs between the Cys5 and Cys55 β-protons in the UL-Cys-labeled BPTI (**a**) and the (L-[β-^{13}C; α,β_2/β_3-$^2H_2$] Cys, [U-^{2}H])-labeled BPTI (**b**). The experimental conditions were the same as those for Fig. 5. The spin diffusion of the NOE was dramatically suppressed in **b**, as compared to **a**. The intensity units in **a** and **b** are arbitrary relative to each other

independently estimated by a ^{13}C T_1/T_2 analysis on the $^{13}C_\beta$ atom of the same sample (Table S2) (Lipari and Szabo 1982a, b; Kojima et al. 1998). The correlation time of the 1.0 mM BPTI sample at 10°C and 14.4 T (^{1}H frequency of 600 MHz) was estimated to be 5.3 ± 0.5 ns. The cross-relaxation rates were then converted to the effective distances.

The estimated effective distances coincided fairly well with the distances in the high-resolution crystal structure of the BPTI protein at a resolution of 1.0 Å (PDB# 5PTI) (Fig. 7b) (Table S3). Although subtle differences were observed between the effective distances and the rigid distances, possibly due to the radial and angular fluctuations of the inter-atom vector (Olejniczak et al. 1984; Brüeschweiler et al. 1992; Lane 1988; Macura et al. 1994), the determined effective distances are certainly valuable for elucidating the disulfide conformations.

One may consider the aforementioned procedures to be difficult, as they require the acquisition of several NOESY spectra at different mixing times and the evaluations of the isotope enrichment and the overall molecular correlation time. A much easier approach is to acquire the NOESY spectrum at a single mixing time using the (L-[β-^{13}C; α,β_2/β_3-$^2H_2$] Cys, [U-^{2}H])-labeled protein and then create the possible angle restraints for the three dihedral angles, based on a comparison between the relative NOE peak intensity and the contour map of the inter-proton distance (Fig. 1b), which eliminates the need to evaluate the isotope enrichment and the overall molecular correlation time. However, the NOE-build up curves are very useful to estimate the spin diffusion contribution to the observed NOEs. By including NOESY data at longer mixing times in the curve fitting, the cross-relaxation rate can reliably be evaluated even for long-distance NOEs, whose intensities are otherwise too weak to evaluate at shorter mixing times.

An analysis of the disulfide bond with conformational dynamics

A somewhat unexpected result was that the effective distance of the Cys14–Cys38 disulfide bond coincided with that of the crystal structure, within experimental error, even though it undergoes conformational fluctuation (Otting et al. 1993; Szyperski et al. 1993; Grey et al. 2003; Shaw et al. 2010). A plausible explanation for this is that the populations of m_{c14} and m_{c38} are very small (i.e., m_{c14}, 1.6% at 7°C; m_{c38}, 1.5% at 4°C) (Otting et al. 1993; Grey et al. 2003), as compared to that of M, and hence the exchange with them does not appreciably affect the cross-relaxation rate.

However, this condition with a highly skewed population does not necessarily occur in general cases, where the influence of the conformational exchange with other sub-conformation(s) on the cross-relaxation rate is not negligible. To analyze a specific sub-conformation under such circumstances, the prerequisites are that the exchange rate is slow on the chemical shift time scale and the chemical shifts of the sub-conformation are resolved from those of the other sub-conformations. Furthermore, the analysis of the build-up curves needs to be limited to the initial region of the NOE build-up curve, in order to minimize the influence of the exchange during the NOE mixing times.

It is interesting that, even though the diagonal peaks of m_{c38} were almost undetectable, the exchange peaks between M and m_{c38} were clearly detected in the NOESY spectrum (Fig. 5b), suggesting the utility of the exchange peaks for analyses of the disulfide kinetics and the low-populated conformations. In this regard, it should be pointed out that the exchange peaks are much more discernible in the (L-[β-^{13}C; α,β_2/β_3-$^2H_2$] Cys, [U-^{2}H])-labeled BPTI, as compared with the UL-Cys-labeled BPTI, indicating that the elimination of the spin diffusion is also favorable for observing the exchange peaks as well as the across-disulfide NOEs (Fig. 5). We have been developing a method for analyzing disulfide isomerization by using the exchange peaks, which will be reported elsewhere.

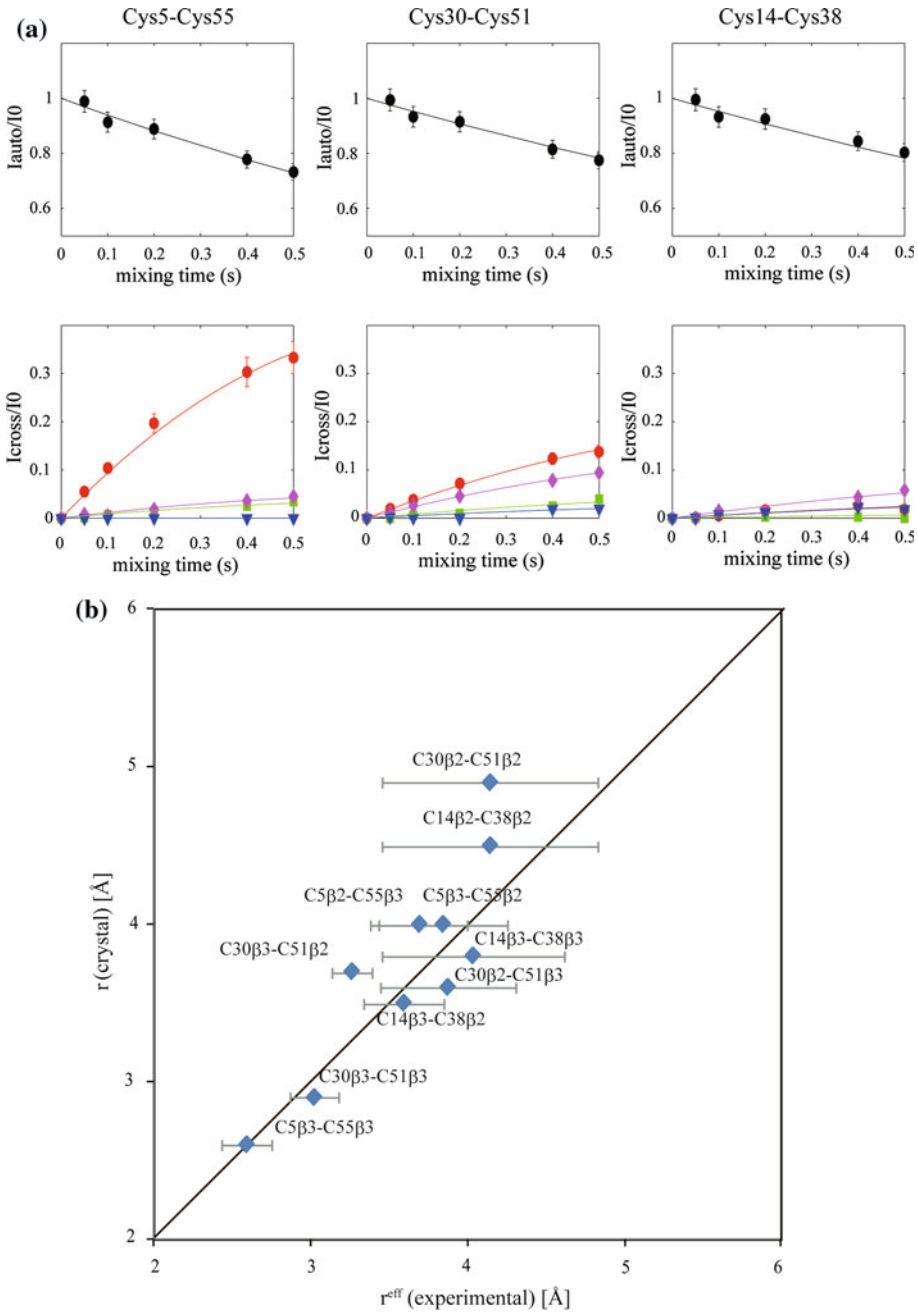

Fig. 7 Intensities of the diagonal peaks and cross-peaks in NOESY spectra as a function of mixing time. The peak intensities are fitted (**a**). The *top panels* show the decay of the diagonal peaks (*black*). The *bottom panels* show the intensities of the across-disulfide NOEs between the *i*th and *j*th Cys residues ($i < j$) [i.e., $H_{\beta 2}(i)$-$H_{\beta 2}(j)$ (*blue*), $H_{\beta 2}(i)$-$H_{\beta 3}(j)$ (*light green*), $H_{\beta 3}(i)$-$H_{\beta 2}(j)$ (*magenta*) and $H_{\beta 3}(i)$-$H_{\beta 3}(j)$ (*red*)]. The determined cross-relaxation rates were converted to the effective inter-proton distances, using an independently determined value of the rotational correlation time of BPTI. The resulting inter-proton distances matched fairly well with those in the crystal structure of BPTI (**b**). These NOESY data were acquired for (L-[β-^{13}C; α ,β_2/β_3-$^2H_2$] Cys, [U-^{2}H])-labeled BPTI. The NOESY experiments were performed at 10°C and a ^{1}H frequency of 600 MHz

Conclusion

We have reported a method for determining disulfide connectivity and conformation, by observing across-disulfide NOEs using a (L-[β-^{13}C; α,β_2/β_3-$^2H_2$] Cys, [U-^{2}H])-labeled protein. As shown in this study, the systematic optimization of the isotope labeling pattern, which is the most important advantage of the SAIL method, provides a chance to obtain structural information that is otherwise quite difficult to investigate. We are currently developing a method for investigating the dynamics of protein disulfide bonds by the SAIL-NMR method.

Acknowledgments This work was supported by the Targeted Proteins Research Program (TPRP) to M. K. and partially by Grants-in-Aid for Young Scientists (B) (21770110, 23770109) to M. T. and a Grant-in-Aid in Innovative Areas (4104) to M. K.

References

Altman JD, Henner D, Nilsson B, Anderson S, Kuntz ID (1991) Intracellular expression of BPTI fusion proteins and single column cleavage/affinity purification by chymotrypsin. Protein Eng 4:593–600

Arnold LD, Kalantar TH, Vederas JC (1985) Conversion of serine to stereochemically pure β-substituted α-amino acids via β-lactones. J Am Chem Soc 107:7105–7109

Arnold LD, May RG, Vederas JC (1988) Synthesis of optically pure α-amino acids via salts of α-amino-β-propiolactone. J Am Chem Soc 110:2237–2241

Berndt KD, Güntert P, Orbons LP, Wüthrich K (1992) Determination of a high-quality nuclear magnetic resonance solution structure of the bovine pancreatic trypsin inhibitor and comparison with three crystal structures. J Mol Biol 277:757–775

Billeter M, Braun W, Wüthrich K (1982) Sequential resonance assignments in protein ^{1}H nuclear magnetic resonance spectra. Computation of sterically allowed proton–proton distances and statistical analysis of proton–proton distances in single crystal protein conformations. J Mol Biol 155:321–346

Boyd J, Hommel U, Campbell ID (1990) Influence of cross-correlation between dipolar and anisotropic chemical shift relaxation mechanisms upon longitudinal relaxation rates of ^{15}N in macromolecules. Chem Phys Lett 175:477–482

Brüeschweiler R, Roux B, Blackledge M, Griesinger C, Karplus M, Ernst RR (1992) Influence of rapid intramolecular motion on NMR cross-relaxation rates. A molecular dynamics study of Antamanide in solution. J Am Chem Soc 114:2289–2302

Cavanagh J, Fairbrother WJ, Palmer AG, Skelton NJ, Rance M (2007) Protein NMR spectroscopy: principles and practice. Academic Press, San Diego

Creighton TE (1984) Disulfide bond formation in proteins. Methods Enzymol 107:305–329

Goerke AR, Swartz JR (2008) Development of cell-free protein synthesis platforms for disulfide bonded proteins. Biotechnol Bioeng 99:351–367

Grey MJ, Wang C, Parmer AG (2003) Disulfide bond isomerization in basic pancreatic trypsin inhibitor: multisite chemical exchange quantified by CPMG relaxation dispersion and chemical shift modeling. J Am Chem Soc 125:14324–14335

Ikeya T, Takeda M, Yoshida H, Terauchi T, Jee JG, Kainosho M, Güntert P (2009) Automated NMR structure determination of stereo-array isotope labeled ubiquitin from minimal sets of spectra using the SAIL-FLYA system. J Biomol NMR 44:261–272

Kainosho M, Güntert P (2009) SAIL—stereo-array isotope labeling. Q Rev Biophys 42:247–300

Kainosho M, Torizawa T, Iwashita Y, Terauchi T, Ono AM, Güntert P (2006) Optimal isotope labelling for NMR protein structure determinations. Nature 440:52–57

Kari C, Nagy Z, Kovács P, Hernádi F (1971) Mechanism of the growth inhibitory effect of cysteine on *Escherichia coli*. J Gen Microbiol 68:349–356

Kay LE, Torchia DA, Bax A (1989) Backbone dynamics of proteins as studied by ^{15}N inverse detected heteronuclear NMR spectroscopy: application to staphylococcal nuclease. Biochemistry 28:8972–8979

Kojima C, Ono A, Kainosho M, James TL (1998) DNA duplex dynamics: NMR relaxation studies of a decamer with uniformly 13C-labeled purine nucleotides. J Magn Reson 135:310–333

Kumar A, Wagner G, Ernst RR, Wüthrich K (1981) Buildup rates of the nuclear Overhauser effect measured by two-dimensional proton magnetic resonance spectroscopy: implications for studies of protein conformation. J Am Chem Soc 103:3654–3658

Lane AN (1988) The influence of spin diffusion and internal motions on NOE intensities in proteins. J Magn Reson 78:425–439

LeMaster DM (1996) Structural determinants of the catalytic reactivity of the buried cysteine of *Escherichia coli* thioredoxin. Biochemistry 35:14876–14881

Lipari G, Szabo A (1982a) Model-free approach to the interpretation of nuclear magnetic resonance relaxation in macromolecules. 1. Theory and range of validity. J Am Chem Soc 104:4546–4559

Lipari G, Szabo A (1982b) Model-free approach to the interpretation of nuclear magnetic resonance relaxation in macromolecules. 2. Analysis of experimental results. J Am Chem Soc 104: 4559–4570

Macura S, Fejzo J, Westler WM, Markley JL (1994) Influence of slow internal motion in proteins on cross-relaxation rates determined by two-dimensional exchange spectroscopy. Bull Magn Reson 16:73–93

Markley JL, Bax A, Arata Y, Hilbers CW, Kaptein R, Sykes BD, Wright PE, Wüthrich K (1998) Recommendations for the presentation of NMR structures of proteins and nucleic acids. J Mol Biol 280:933–952

Matsumura M, Matthews BW (1991) Stabilization of functional proteins by introduction of multiple disulfide bonds. Methods Enzymol 202:336–356

Miyanoiri Y, Takeda M, Jee J, Ono AM, Okuma K, Terauchi T, Kainosho M (2011) Alternative SAIL-Trp for robust aromatic signal assignment and determination of the χ(2) conformation by intra-residue NOEs. J Biomol NMR. doi:10.1007/s10858-011-9568-3 (in press)

Mobli M, King GF (2010) NMR methods for determining disulfide-bond connectivities. Toxicon 56:849–854

Mobli M, de Araújo AD, Lambert LK, Pierens GK, Windley MJ, Nicholson GM, Alewood PF, King GF (2009) Direct visualization of disulfide bonds through diselenide proxies using ^{77}Se NMR spectroscopy. Angew Chem Int Ed Engl 48:9312–9314

Muchmore DC, McIntosh LP, Russell CB, Anderson DE, Dahlquist FW (1989) Expression and nitrogen-15 labeling of proteins for proton and nitrogen-15 nuclear magnetic resonance. Methods Enzymol 177:44–73

Olejniczak ET, Dobson CM, Karplus M, Levy RM (1984) Motional averaging of proton nuclear overhauser effects in proteins. Predictions from a molecular dynamics simulation of lysozyme. J Am Chem Soc 106:1923–1930

Otting G, Liepinsh E, Wüthrich K (1993) Disulfide bond isomerization in BPTI and BPTI (G36S): an NMR study of correlated mobility in proteins. Biochemistry 32:3571–3582

Ozhogina OA, Bominaar EL (2009) Characterization of the kringle fold and identification of a ubiquitous new class of disulfide rotamers. J Struct Biol 168:223–233

Peng JW, Wagner G (1992) Mapping of spectral density functions using heteronuclear NMR relaxation measurements. J Magn Reson 98:308–322

Ramer SE, Moore RN, Vederas JC (1986) Mechanism of formation of Serine β-lactones by Mitsunobu cyclization: synthesis and use of L-Serine stereospecifically labelled with deuterium at C-3. Can J Chem 64:706

Richardson JS (1981) The anatomy and taxonomy of protein structure. Adv Prot Chem 34:167–339

Roberts RB, Abelson PH, Cowie DB, Bolton ET, Britten RJ (1957) Studies of biosynthesis in *Escherichia coli*, vol 607. Carnegie Institution of Washington Publications, Washington

Schmidt B, Hogg PJ (2007) Search for allosteric disulfide bonds in NMR structures. BMC Struct Biol 7:49

Schmidt B, Ho L, Hogg PJ (2006) Allosteric disulfide bonds. Biochemistry 45:7429–7433

Shaw DE, Maragakis P, Lindorff-Larsen K, Piana S, Dror RO, Eastwood MP, Bank JA, Jumper JM, Salmon JK, Shan Y, Wriggers W (2010) Atomic-level characterization of the structural dynamics of proteins. Science 330:341–346

Skalicky JJ, Mills JL, Sharma S, Szyperski T (2001) Aromatic ring-flipping in supercooled water: implications for NMR-based structural biology of proteins. J Am Chem Soc 123:388–397

Szyperski T, Luginbühl P, Otting G, Güntert P, Wüthrich K (1993) Protein dynamics studied by rotating frame ^{15}N spin relaxation times. J Biomol NMR 3:151–164

Takahashi H, Kainosho M, Akutsu H, Fujiwara T (2010) ^{1}H-detected ^{1}H-^{1}H correlation spectroscopy of a stereo-array isotope labeled amino acid under fast magic-angle spinning. J Magn Reson 203:253–256

Takeda M, Ikeya T, Güntert P, Kainosho M (2007) Automated structure determination of proteins with the SAIL-FLYA NMR method. Nat Protoc 2:2896–2902

Takeda M, Jee J, Ono AM, Terauchi T, Kainosho M (2009) Hydrogen exchange rate of tyrosine hydroxyl groups in proteins as studied by the deuterium isotope effect on Cζ chemical shifts. J Am Chem Soc 131:18556–18562

Takeda M, Terauchi T, Ono AM, Kainosho M (2010a) Application of SAIL phenylalanine and tyrosine with alternative isotope-labeling patterns for protein structure determination. J Biomol NMR 46:45–49

Takeda M, Jee J, Terauchi T, Kainosho M (2010b) Detection of the sulfhydryl groups in proteins with slow hydrogen exchange rates and determination of their proton/deuteron fractionation factors using the deuterium-induced effects on the ^{13}Cβ NMR signals. J Am Chem Soc 132:6254–6260

Takeda M, Jee J, Ono AM, Terauchi T, Kainosho M (2011) Hydrogen exchange study on the hydroxyl groups of Serine and Threonine residues in proteins and structure refinement using NOE restraints with polar side-chain groups. J Am Chem Soc 133: 17420–17427

Terauchi T, Kobayashi K, Okuma K, Oba M, Nishiyama K, Kainosho M (2008) Stereoselective synthesis of triply isotope-labeled Ser, Cys, and Ala: amino acids for stereoarray isotope labeling technology. Org Lett 10:2785–2787

Torizawa T, Shimizu M, Taoka M, Miyano H, Kainosho M (2004) Efficient production of isotopically labeled proteins by cell-free synthesis: a practical protocol. J Biomol NMR 30:311–325

Vögeli B, Segawa TF, Leitz D, Sobol A, Choutko A, Trzesniak D, van Gunsteren W, Riek R (2009) Exact distances and internal dynamics of perdeuterated ubiquitin from NOE buildups. J Am Chem Soc 131:17215–17225

Vögeli B, Friedmann M, Leitz D, Sobol A, Riek R (2010) Quantitative determination of NOE rates in perdeuterated and protonated proteins: practical and theoretical aspects. J Magn Reson 204:290–302

Wagner G (1983) Characterization of the distribution of internal motions in the basic pancreatic trypsin inhibitor using a large number of internal NMR probes. Q Rev Biophys 16:1–57

Walewska A, Skalicky JJ, Davis DR, Zhang MM, Lopez-Vera E, Watkins M, Han TS, Yoshikami D, Olivera BM, Bulaj G (2008) NMR-based mapping of disulfide bridges in cysteine-rich peptides: application to the mu-conotoxin SxIIIA. J Am Chem Soc 130:14280–14286

Waugh DS (1996) Genetic tools for selective labeling of proteins with alpha-^{15}N-amino acids. J Biomol NMR 8:148–192

Wlodawer A, Walter J, Huber R, Sjölin L (1984) Structure of bovine pancreatic trypsin inhibitor. Results of joint neutron and X-ray refinement of crystal form II. J Mol Biol 180:301–329

Wu J, Fan J, Pascal SM, Yang D (2004) General method for suppression of diagonal peaks in heteronuclear-edited NOESY spectroscopy. J Am Chem Soc 126:15018–15019